

# Mechanical properties of mammalian single smooth muscle cells

## III. Passive properties of pig detrusor and human a terme uterus cells

J. J. GLERUM\*, R. VAN MASTRIGT and A. J. VAN KOEVERINGE

Departments of Urology and Biomedical Physics and Technology, Erasmus University Rotterdam, The Netherlands

Received 14 May 1990; accepted 6 June 1990

### Summary

Cells isolated from pig urinary bladders and pregnant full term human uteruses were attached longitudinally between a microforce transducer and a length displacement apparatus. Cells were stretched by applying a series of ramp-like length changes of 0.2 s duration and 10.0  $\mu\text{m}$  amplitude at intervals of 15 min. Passive forces upon straining were as high as 70–100  $\mu\text{N}$ . Following these peak forces stress relaxation occurred, levelling off approximately 50% of the maximum peak force. The maximum elastic modulus estimated for single cells was found to be at least a tenfold higher than was previously estimated from intact bladder strips. The relation between the increase in length and the increase in initial force increment was found to be approximately linear. An exponential equation was fitted to a selected number of stress relaxation curves. Relaxation curves of bladder cells show a clearly different time course as compared to bladder tissue strips, suggesting that a significant amount of relaxation in strips has to be contributed to the connective tissue components or to structural changes in these strips.

### Introduction

The bladder in its filling phase and the growing uterus in the course of pregnancy show a remarkable increase in diameter and volume. For the bladder this increase in volume is solely attributed to passive stretching of connective and muscle tissue (Van Mastrigt *et al.*, 1978). The uterus not only shows passive elongation of its tissue components, but also growth, e.g. multiplication and hypertrophy of its smooth muscle cells (Ham, 1974). The time course of relaxation in bladder tissue has been shown to be clinically relevant (Coolsaet, 1977; Kondo & Susset, 1972; Van Mastrigt *et al.*, 1981; Susset & Regnier, 1981). Incompetence of the cervix in the first and second trimester of pregnancy seems to be related to a different passive and/or active behaviour of uterine smooth muscle (Drogendijk *et al.*, 1988; Van der Zon *et al.*, 1989).

In both cases it is difficult to relate measurements performed on large preparations to mechanisms at the cellular level. In this study the passive properties of single smooth muscle cells are reported. The pig urinary bladder was used as a well accepted model for the human urinary bladder (Douglas, 1972). The very small amounts of tissue necessary for single cell experiments with uterine muscle cells were obtained at Caesarean sections, without inter-

ference with either the procedure or with the mother's and child's interests.

### Materials and methods

Single smooth muscle cells from pig urinary bladders were isolated by enzymatic digestion of strips of bladder tissue collected at the local slaughterhouse.

Single smooth muscle cells from a terme human uteruses were obtained likewise from biopsies excised at Caesarean sections. Both procedures were carried out as described previously (Glerum *et al.*, 1987; Glerum & Van Mastrigt, 1990b).

The cells were incubated in a cell incubator mounted on a Zeiss inverted microscope, equipped with phase contrast and incident light fluorescence optics. Conditions of incubation were kept at temperature 37°C;  $\text{pO}_2$  150 mm Hg and  $\text{pCO}_2$  38 mm Hg approximately, thus resulting in pH 7.35 (Glerum *et al.*, 1987).

Cells in suspension were checked for vitality by means of an FDA fluorescence vital staining technique and selected vital cells were knotted between two micropipettes attached to a length displacement apparatus and a micro force transducer (sensitivity 10  $\mu\text{N V}^{-1}$ ) as depicted before (Glerum & Van Mastrigt, 1990a, b).

\*Author to whom correspondence should be addressed at: Department of Urology, Erasmus University, Room EE 1630, P.O. Box 1738, 3000 DR Rotterdam, The Netherlands.

Subsequently cells were stretched to resting or initial length by applying one or more ramp-like length increments of  $10\mu\text{m}$  amplitude and 0.2 s duration until a rise in force directly followed by visco-elastic relaxation was recorded. The free cell length between the knots was optically measured through the microscope at this moment and was defined and recorded as the initial length  $L_1$ .

After an initial resting period of 15 min, cells were stretched by applying further ramp stretches of  $10\mu\text{m}$  amplitude at intervals of 15 min until they broke.

The microforce transducer output signal, showing both the peak force and the stress-relaxation behaviour of the cell, was sampled at 10 Hz during 90 s by a PDP11 type computer, starting 10 s before the start of each length increment. The obtained data were stored on hard disk for analysis. Figure 1 shows a schematic diagram of the measurement apparatus.

The stored stress relaxation curves were analysed as follows: every curve, one at a time, was displayed at the computer screen and cursors were placed at the force levels corresponding to force before stretching ( $F_1$ ), maximum peak force during the

ramp ( $F_2$ ) and force after 80 s of relaxation ( $F_3$ ).  $F_2$  minus  $F_1$  was called  $dF$ , and the percentage of force ( $rF\%$ ) remaining after 80 s relaxation was calculated as:

$$rF\% = (F_3 - F_1)/(F_2 - F_1) \times 100\% \quad (1)$$

Plots of  $dF$  versus length were made for each cell, and the slope of the rising part of the curve ( $\alpha$  = chord stiffness) was estimated:

$$\alpha = (dF_2 - dF_1)/(L_2 - L_1) \quad (2)$$

where

$L_1$  = cell length at the onset of the approximately linear rise of  $dF$  with  $L$

$L_2$  = cell length at the end of the approximately linear rise of  $dF$  with  $L$

$dF_1$  =  $dF$  value corresponding with  $L_1$

$dF_2$  =  $dF$  value corresponding with  $L_2$ .

The definition of the elastic modulus  $E$ :

$$E = \Delta\sigma/\Delta\varepsilon \quad (3)$$

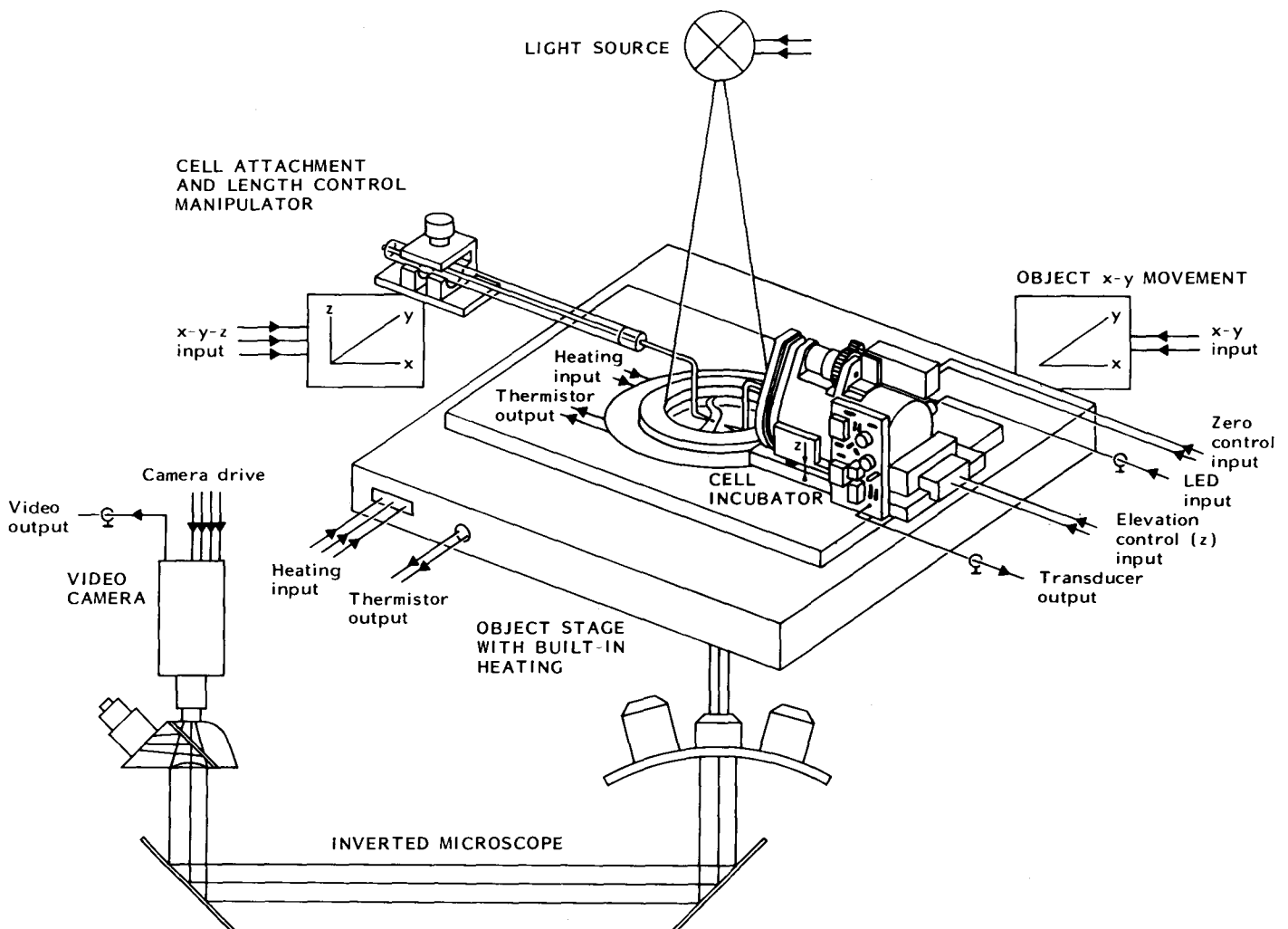


**Fig. 1.** Schematic diagram of the measurement apparatus. The diagram shows the cell incubation bath mounted on the object table of an inverted microscope. To the right of the cell incubator an ultrasensitive force transducer is mounted on a specially designed elevation control mechanism. Left of the cell incubator a three-dimensional micromanipulator, serving as a length control apparatus, is attached to the object table. Micropipettes attached to the transducer and the micromanipulator are bent in a Z-like form to overcome the differences in height and distance from the transducer and the micromanipulator to the actual spot where the cell is situated in the incubation bath.

where

- E = elastic modulus
- $\Delta\sigma$  = increase in stress
- $\Delta\varepsilon$  = increase in strain

was rewritten in the form:

$$E = (\Delta F/A) \times (L/\Delta L) \tag{4}$$

where

- $\Delta F$  = increase in force
- A = crosssectional area
- L = length
- $\Delta L$  = change in length.

Assuming a cell to be a cylinder with a constant volume  $V_i$ :

$$V_i = \pi r_i^2 \times L_i = A \times L \tag{5}$$

where

- $r_i$  = the radius of the cell at resting length
  - $L_i$  = resting length.
- This yields:

$$E = \Delta F \times L^2 / (\pi r_i^2 \times L_i \times \Delta L) \tag{6}$$

For comparison of elastic moduli determined in this way with moduli calculated from experiments on larger preparations the value of Equation (6) at maximum cell length ( $E_{max}$ ) was taken:

$$E_{max} = dF_{max} \times L_{dF_{max}}^2 / (\pi r_i^2 \times L_i \times \Delta L) \tag{7}$$

where

- $E_{max}$  = the maximum elastic modulus at maximum length
- $L_{dF_{max}}$  = the cell's length obtained at the ultimate length increment where the cell still remained intact
- $\Delta L$  = amplitude of the ramp stretch.

The radius of the cell at initial length,  $r_i$ , was estimated optically.

The following parameters were tested for reproducibility: the cell length prior to the (first) decrease in  $dF$  ( $L_{pd}$ ),  $dF$  prior to decrease in  $dF$  ( $dF_{pd}$ ) and the absolute force prior to decrease in  $dF$  ( $F_{apd}$ ). Also the absolute force ( $F_{break}$ ) and length ( $L_{break}$ ) at the moment of breaking were estimated.

To quantify the process of stress relaxation to a number of curves an exponential function of the form:

$$F(t) = C_1 e^{B_1 t} + C_2 \tag{8}$$

was fitted using a Marquardt iterative procedure (Kirkegaard, 1970).

Only curves that showed a continuous decrease in force without intermediate dips or peaks greater than 1.5  $\mu N$  deviation during at least 70 s, were considered correctly fitted curves.

Differences in variables were tested for significance using the Mann-Whitney U-test, at a significance level of 10%.

### Results

In 19 experiments 12 pig urinary bladder smooth muscle cells and six human uterus smooth muscle cells were attached to the measuring apparatus and stepwise stretched until they broke. One pig urinary bladder cell accidentally broke at small length, due to wrong micro-manipulations. Figure 2 shows a typical example of a stress relaxation curve, and the measured variables  $F_1$ ,  $F_2$

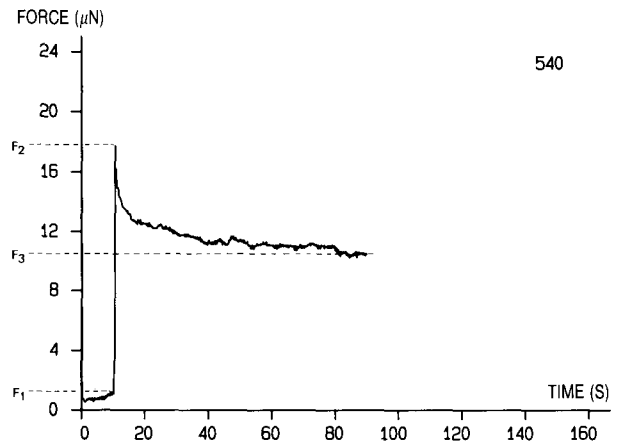


**Fig. 2.** A typical example of a stress relaxation curve measured in response to a 10  $\mu m$  stepwise length increase of a human uterus smooth muscle cell.  $F_1$  indicates the force level just prior to the length step,  $F_2$  indicates the maximum force level at the moment of the length step and  $F_3$  indicates the force level after 80 s of stress relaxation. Stretched cell length between the knots was 95  $\mu m$ .

and  $F_3$ . Eighty-six such curves were obtained from the bladder cells and 53 from the uterus cells.

For all cells  $dF$  was plotted as a function of length. A total of 13 out of these 19 curves showed a continuous increase in  $dF$  with increasing length, except for a final discontinuity just before the cell broke. Figure 3 shows an example of this pattern. This same figure also illustrates how the slope of the curve was estimated from the linear part of the curve. One curve of a bladder cell was too

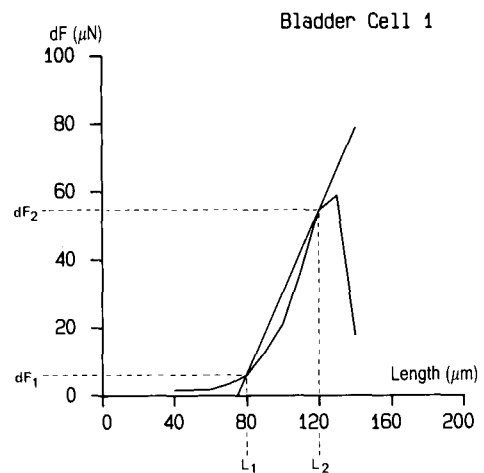


**Fig. 3.** A typical example of the change in the initial force increment ( $dF$ ), resulting from stepwise straining of a bladder smooth muscle cell, as a function of cell length.  $L_1$  indicates the onset of the linear segment of the curve and  $dF_1$  is the corresponding force increment.  $L_2$  indicates the end of the linear segment, with its corresponding force increment  $dF_2$ . The slope of the straight line ( $L_1$ ,  $dF_1$ ) to ( $L_2$ ,  $dF_2$ ) was calculated as  $\alpha$ . The curve shows an abrupt decrease in  $dF$ , indicating the maximum range of cell lengthening. At a stretched length of 140  $\mu m$  the cell broke.

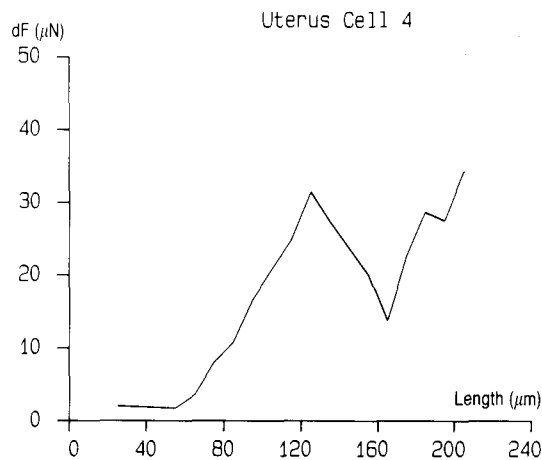


Fig. 4. An example of the change in  $dF$  as a function of length for a uterine smooth muscle cell showing two dips in the increment of  $dF$  before the cell broke.

short to allow further analysis (cell 12), two uterus cells showed one additional discontinuity in  $dF$  increment and three bladder cells showed two or more discontinuities in the increment of  $dF$  with length. Figure 4 shows  $dF$  versus length for one of the few cells that showed repeated dips in  $dF$  increment.

$F_3$  (remaining steady force after 80 s of relaxation) versus length was also plotted for the same cells. As this pattern grossly paralleled that of  $dF$  versus length (see Fig. 5) further data on  $F_3$  are not presented here and analysis was concentrated on  $dF$  and other variables.

As Tables 1 and 2 show, the average initial length ( $L_i$ ) was  $34 \mu\text{m}$  for bladder cells and  $29 \mu\text{m}$  for uterus cells. This length is the free length between the knots on the

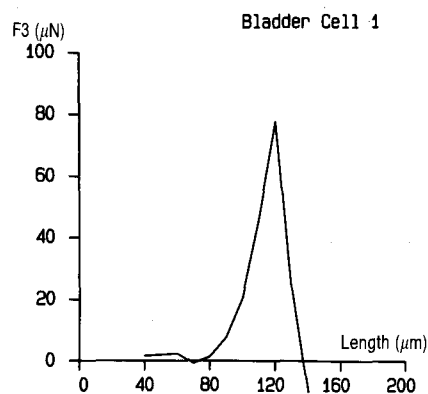


Fig. 5. A typical example of the change in  $F_3$ , remaining steady force after 80 s of relaxation, resulting from stepwise straining of a bladder smooth muscle cell, as a function of cell length. At a stretched length of  $140 \mu\text{m}$  the cell broke.

micropipettes. A considerable part of the cellbody ( $20\text{--}30 \mu\text{m}$  for each knot) was used for the knots.

The average slope ( $\alpha$ ) of the approximately linear increase of  $dF$  with length was  $0.52 \mu\text{N} \mu\text{m}^{-1}$  for bladder cells and  $0.28 \mu\text{N} \mu\text{m}^{-1}$  for uterus cells.

Both types of cells showed a levelling off of relaxation at approximately the same average remaining strain level ( $rF\%$ ) of 51 and 55% respectively. The average maximum elastic modulus ( $E_{\text{max}}$ ) values were also similar, at  $11.0$  and  $12.2 \times 10^6 \text{ N m}^{-2}$  respectively.

The moment at which a discontinuity in increase of  $dF$  with length occurred did not seem to be uniquely related to either length,  $dF$  or absolute force, as is shown in columns 1, 2 and 3 of Tables 3 and 4. These show, for the same cells as in Tables 1 and 2, length ( $L_{\text{pd}}$ ),  $dF$  ( $dF_{\text{pd}}$ ) and

Table 1. Passive properties of pig urinary bladder smooth muscle cells.

Cell no.	$L_i$ ( $\mu\text{m}$ )	$\alpha$ $\text{N m}^{-1}$	$rF\%$ %	SEM*	$E_{\text{max}}$ $\text{N m}^{-2} \times 10^{-6}$
1	40	0.64	50.0	9.4	31.7
2	40	0.33	46.0	8.4	4.6
3	40	0.05	78.6	—	1.2
4	30	0.56	44.2	8.2	10.7
5	25	0.24	63.1	2.9	19.9
6	25	0.87	46.2	8.3	13.1
7	30	0.18	32.6	5.0	6.6
8	25	0.39	55.8	6.2	11.8
9	40	1.94	69.8	12.5	15.0
10	30	0.17	53.2	15.9	0.5
11	25	0.66	65.1	5.5	12.7
12	45	—	32.0	14.2	—
13	50	0.23	48.8	5.4	4.7
mean	34.2	0.52	50.9		11.0
SEM*	2.4	0.15	2.4		2.5

$L_i$  = initial length;  $\alpha$  = the slope of the increase of  $dF$  with length;  $rF\%$  = the average remaining force after 80 s of relaxation;  $E_{\text{max}}$  = the maximum elastic modulus.

\* Standard error of mean.

**Table 2.** Passive properties of human a terme uterine smooth muscle cells.

Cell no.	$L_i$ ( $\mu\text{m}$ )	$\alpha$ $\text{N m}^{-1}$	$rF\%$ %	SEM*	$E_{max}$ $\text{N m}^{-2} \times 10^{-6}$
1	30	0.22	67.0	2.7	12.7
2	30	0.39	51.3	3.0	8.4
3	50	0.15	49.9	2.8	10.3
4	25	0.42	54.1	3.7	25.0
5	20	0.22	42.8	4.9	6.1
6	20	0.29	57.8	5.6	10.8
mean	29.2	0.28	54.6		12.2
SEM*	4.5	0.04	1.9		2.7

$L_i$  = initial length;  $\alpha$  = the slope of the increase of  $dF$  with length;  $rF\%$  = the average remaining force after 80 s of relaxation;  $E_{max}$  = the maximum elastic modulus.

\* Standard error of mean.

**Table 3.** Passive properties of pig urinary bladder smooth muscle cells.

Cell no. (n)	$L_{pd}$ ( $\mu\text{m}$ )	$dF_{pd}$ ( $\mu\text{N}$ )	$F_{apd}$ ( $\mu\text{N}$ )	$L_{break}$ ( $\mu\text{m}$ )	$F_{break}$ ( $\mu\text{N}$ )
1	130	58.9	122.0	140	90.7
2	90	17.7	21.6	100	22.2
3	100	3.7	9.0	110	5.2
4	50 (60/90/120)	14.7	14.0	130	23.7
5	125	25.0	60.6	135	63.2
6	75 (85/95) (115/125/135)	45.6	115.3	155	90.9
7	80 (90/110)	10.1	10.8	120	13.2
8	75	17.1	42.6	115	76.3
9	60	41.6	44.1	80	160.0
10	50	4.3	10.4	80	6.4
11	75	34.2	40.3	85	75.0
13	100	11.9	15.4	120	18.8
average	84.2	23.7	42.2	114.2	53.8
SEM*	7.5	5.1	11.4	7.0	13.6

$L_{pd}$  = the cell length prior to the length at which the (first) discontinuity in increase of  $dF$  with increase in length occurred (figures in brackets indicate lengths at which such a discontinuity, if more than once, occurred);  $dF_{pd}$  =  $dF$  prior to the (first) discontinuity;  $F_{apd}$  = absolute force prior to the (first) discontinuity;  $L_{break}$  = length at which the cell broke;  $F_{break}$  = absolute force at which the cell broke.

\* Standard error of mean.

absolute force ( $F_{apd}$ ) as calculated from the stretch response prior to the first stretch at which such a discontinuity was observed. If any of the following stretches showed another discontinuity in  $dF$  increment, the lengths at which these occurred are printed in small print in column 1 of both Tables.

Graphical analysis of the data in Tables 1–6 showed that all parameter values could be considered as properly fitting in a continuum of values. Therefore, in all further analysis and statistics, cells of the same organ type were treated as one homogeneous group and differences in variables were only tested between bladder and uterus cells.

Although averages obtained for most variables in Tables 1–4 seem to show differences between bladder and uterus cells, none of these differences proved to be significant according to the Mann-Whitney U-test at a significance level of 10%. If, however, cells 2 and 3, which showed many wavelike force increases superimposed on their relaxation curves, and cell 10, which was very thin at one of its ends, are excluded from the bladder cell results, the difference in  $\alpha$  between bladder and uterus cells (0.64 and 0.28 respectively) becomes significant ( $p = 0.077$ ).

Figure 6 shows a typical example of a fitted stress relaxation curve describing the relaxation behaviour within the displayed time window. A significant number of the

**Table 4.** Passive properties of human a terme uterus smooth muscle cells.

Cell no. (n)	$L_{pd}$ ( $\mu m$ )	$dF_{pd}$ ( $\mu N$ )	$F_{apd}$ ( $\mu N$ )	$L_{break}$ ( $\mu m$ )	$F_{break}$ ( $\mu N$ )
1	120	20.8	38.9	130	41.6
2	80	18.2	23.5	90	50.8
3	110 (120/170)	10.7	22.7	180	30.2
4	125 (135/185)	31.5	69.0	205	81.1
5	50	8.0	11.5	90	25.3
6	90	20.9	55.0	110	44.8
average	95.8	18.3	36.8	134.2	45.6
SEM*	11.6	3.4	8.9	19.7	8.1

$L_{pd}$  = the cell length prior to the length at which the (first) discontinuity in increase of  $dF$  with increase in length occurred (figures in brackets indicate lengths at which such a discontinuity, if more than once, occurred);  $dF_{pd}$  =  $dF$  prior to the (first) discontinuity;  $F_{apd}$  = absolute force prior to the (first) discontinuity;  $L_{break}$  = length at which the cell broke;  $F_{break}$  = absolute force at which the cell broke.  
\* Standard error of mean.

relaxation curves, especially in bladder cells, showed increases of force superimposed on the relaxation patterns. In a small number of curves the initial force step was out of range, or accidental mechanical disturbances during the sampling of relaxation had occurred. As these curves could not be fitted with Equation 4 only a limited number of curves, 28 from bladder cells (i.e. 33%) and 34 from uterus cells (i.e. 64%), proved smooth and long enough to allow the exponential curve fitting. The resulting parameters are shown in Tables 5 and 6. In Table 5 no results are shown for bladder cells 2, 3, 4 and 9, as these cells displayed too many or too large superimposed force increases (see discussion) in all relaxation curves. The uterus cells, as shown in Table 6, showed hardly any of

these force increases; a few curves showed short duration peaks smaller than  $0.5 \mu N$ .

It was observed that in almost all cells of either type the last and sometimes also the last but one relaxation curve before cell breakage differed from the preceding ones, sometimes in such a way that a two exponential fitting was considerably better than the routinely applied one exponential fitting. The parameters from the most deviant of these curves were excluded from the averages per cell.

On average, bladder cells did not differ significantly from uterus cells in terms of the exponent ( $-0.0094$  versus  $-0.011$ ), and although average coefficients and constants seemed to be larger for bladder cells than for uterus cells ( $5.71$  and  $14.0$  versus  $4.50$  and  $9.4$  respectively), these differences were not significant according to the Mann-Whitney U-test.

## Discussion

Anatomically, the urinary bladder does not seem structurally organized: throughout the whole bladder circumference muscle cell bundles are seen to be diverting in all possible directions and converging again from all directions (Gosling *et al.*, 1983). There is no clear distinction between circular and/or longitudinal muscle layers, and the connective tissue components such as collagen, elastin and reticulin seem distributed randomly. The bladder wall must therefore be considered as homogeneous. In contrast, the uterus shows a rather organized structure. Muscle cells are organized in parallel and three ill-defined layers can be discerned. The outer and innermost layers are longitudinally and obliquely orientated; the thickest, middle layer shows a circular orientation and contains the larger blood vessels of the uterus (Ham, 1974).

**Table 5.** Results of fitting the stress relaxation curves of pig urinary bladder smooth muscle cells with an exponential function.

Cell no.	N	Coefficient ( $\mu N$ )	SEM*	Exponent ( $s^{-1}$ )	SEM*	Constant ( $\mu N$ )	SEM*
1	4	8.54	2.39	-0.017	0.0099	39.3	15.1
5	3	1.83	0.69	-0.0095	0.0081	14.08	8.6
6	7	13.19	5.11	-0.0078	0.0016	12.1	2.2
8	1	2.61	—	-0.0065	—	21.2	—
10	2	0.90	0.31	-0.0041	0.00007	3.5	0.4
11	3	3.48	1.72	-0.0076	0.00087	13.8	6.2
12	2	0.32	0.041	-0.012	0.0029	2.0	1.4
13	6	2.059	0.59	-0.010	0.0030	5.8	1.1
average		5.71		-0.0098		14.0	
SEM*		1.57		0.0017		3.1	

N = number of stress relaxation curves fitted per cell; columns 3, 4 and 5 show averages and SEM for respectively the coefficient, exponent and constant of the fitted curves per cell; bottom lines show overall averages and SEM for the same variables of all adequately fitted curves.

\* Standard error of mean.

**Table 6.** Results of fitting the stress relaxation curves of human a terme uterine smooth muscle cells with an exponential function.

Cell no.	N	Coefficient ( $\mu\text{N}$ )	SEM*	Exponent ( $\text{s}^{-1}$ )	SEM*	Constant ( $\mu\text{N}$ )	SEM*
1	4	3.25	1.29	-0.0055	0.0021	12.3	2.6
2	3	2.68	1.14	-0.011	0.0033	8.1	2.0
3	6	2.30	0.62	-0.0070	0.0020	7.1	1.4
4	8	8.060	1.64	-0.013	0.0027	13.4	1.1
5	6	1.85	0.31	-0.0082	0.0032	6.4	1.1
6	7	6.067	2.52	-0.017	0.0045	8.5	1.2
average		4.50		-0.011		9.4	
SEM*		0.77		0.0014		0.7	

N = number of stress relaxation curves fitted per cell; columns 3, 4 and 5 show averages and SEM for respectively the coefficient, exponent and constant of the fitted curves per cell; bottom lines show overall averages and SEM for the same variables of all adequately fitted curves.

\* Standard error of mean.

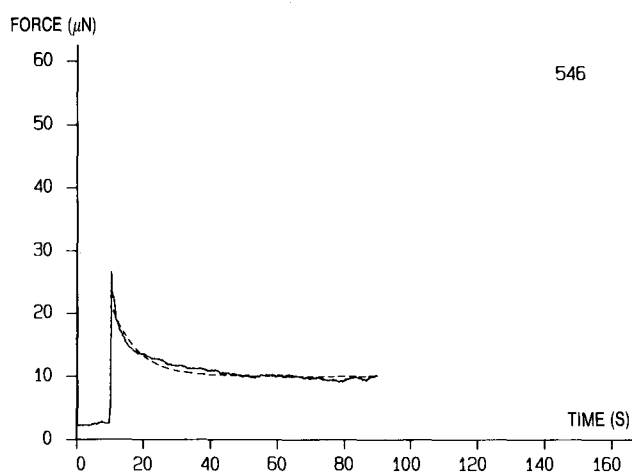


**Fig. 6.** A typical example of a stress relaxation curve measured in response to a  $10\ \mu\text{m}$  stepwise length increase of a human uterus smooth muscle cell to which a one exponential function was fitted. The dotted curve indicates the fitted exponential function. Stretched cell length between the knots was  $115\ \mu\text{m}$ .

The passive properties of smooth muscle cells play a significant role in a number of clinical problems. For instance in the filling phase of cystometry, where distended urinary bladders show low elasticity and large filling volumes. Regarding the uterus, passive properties of the cervix are clinically measured in relation to incompetence of the cervix. Although the cervix consists mainly of connective tissue components, it is also directly related to the lower segment of the uterus which consists mainly of smooth muscle. The latter might therefore play a role in the stable closure of the uterus until the moment of birth (Drogendijk *et al.*, 1988; Van der Zon *et al.*, 1989).

For a clinical evaluation of the relevance of the above outlined mechanisms, measurements of the passive properties of smooth muscle biopsies of these tissues are necessary. In the present study the passive properties of

supposedly normal smooth muscle cells are discussed. As in both *in vivo* and *in vitro*, and even in single cells, there is the possibility of active processes underlying so called passive phenomena, we limit our definition of passive properties to those properties that can reasonably be described or explained by well known passive physical processes such as visco-elasticity.

Microanatomically a smooth muscle cell is not homogeneous but contains obliquely orientated contractile filaments anchored with dense bodies to the cell membrane. In the contractile filaments dense bodies are also seen which are thought to be transversely interconnected by intermediated filaments forming a cyto-skeleton (Squire, 1981; Stephens, 1984).

In a completely passive cell, therefore, the phenomena recorded in our experiments would reflect the properties of the cyto-skeleton in combination with those of the cell membrane. As, on the other hand, in these experiments no special measures were taken to exclude activation of the cell, passive and even active components of the contractile apparatus might contribute to the stress-relaxation recordings.

In the theoretical situation of a totally inactive contractile mechanism, repeated stepwise straining of the cell would result in successive uninterrupted steep rises in force upon stretching followed by a smooth exponential decay of force to a basic level. If, on the other hand, the cell actively maintains force by a continuous cycling of cross-bridges, it would show a sudden initial drop in force upon stretching it past the range of the cross-bridges (approximately 2–4% of muscle length [Van Mastrigt, 1988]). Force recovery would then occur as a result of cross-bridge cycling with a time constant in the order of 2.2 s (Van Mastrigt, 1989). The force relaxation curve in this case would not be convex towards the time axis, as is the case in passive stress relaxation.

An alternative that should be considered is that the cells maintain force through dephosphorylated cross-

bridges, in a low energy or 'latch' state (Marston, 1989). In such a case the stretch amplitudes applied in our experiments would also lead to detachment of these latch-bridges and any further influence of latch-bridges in the following stretches and relaxations would require recycled latch-bridges. Recent evidence (Hai & Murphy, 1988a,b) suggests that there is only one way to reattach latch-bridges after pulling them apart: by the normal sequence of actine-myosine interaction, including the steps of phosphorylation and dephosphorylation. Therefore, latch-bridge reattachment would also result in rather steep rises in force or, as stated before, in case of stretch followed by relaxation, the relaxation curve would not be convex towards the time axis. This still leaves the possibility that the very first measurements made on each cell showed a considerable overestimation of  $dF$ , due to pre-existing latch-bridges, as possibly induced by, for example, depolarization during the isolation and knotting procedures. Since, however none of the  $dF$  versus length curves (see Fig. 3) showed a significantly higher  $dF$  value at the very first stretch, latch-bridge activity in these measurements could be ruled out.

For the data presented, typical stress relaxation curves were obtained in most cases as depicted in Fig. 2. In those cases where (small) wavelike increments of force were superimposed on the relaxation curves, the delay between the stretch and the onset of a superimposed force rise varied from at least 10–30 s, probably indicating a stretch induced cell depolarization, which gave rise to an additive active force component on the passive relaxation curve. In intact bladder muscle, and in bladder strips, the effects of stretch activated cell depolarization leading to force increases by cross-bridge cycling, were observed approximately 40–60 s after rapidly stretching the muscle (Levin *et al.*, 1986; Van Mastrigt, 1977). The resulting wave-like superimposed force increments on the relaxation curve did not affect the general form of the relaxation curve to a significant degree (Coolsaet, 1975b). In this study only bladder cells 2 and 3 showed superimposed force waves of such a magnitude (approximately 2–3  $\mu\text{N}$  peak to peak) that this behaviour was reflected in the results of Tables 1 and 4.

In a limited number of pilot experiments, the contractile apparatus was inactivated by incubating the cells in a calcium-free solution containing EGTA after twice rinsing them in the same solution (unpublished data). In these calcium-free cells, wave-like force increments were not clearly observed but the stress-relaxation behaviour remained the same, resulting in comparable time constants.

We conclude that none, or very limited, contractile activity was present in the described measurements, so that Tables 1 to 6 correctly describe these in terms of passive mechanisms.

Apart from bladder cells 2 and 3, previously mentioned, the results in Tables 1 to 4 show a good reproducibility considering the range of forces measured. Bladder cell 10 yielded deviating data as it had only a

very thin part of one of its ends knotted to a microtool. Uterine cells showed an even better reproducibility, which can be ascribed to the far less aggressive isolation method applied, using only collagenase, and the fact that almost none of these cells showed force increases superimposed on the relaxation curves within the observation time window.

Tables 3 and 4 describe the sudden decreases in increment of  $dF$  and the stretch limits of the cells. In the data presented all curves showed, at the final stretch or at the last but one, that a certain limit was reached as the increment of  $dF$  declined or reversed. These last stretches before the cells broke showed a different relaxation pattern which could not always adequately be described by a one exponential function. This indicates that physical changes did occur in the cells at the ultimate level of strain.

The levelling off in  $dF$  versus length curves occurred at a cell length of 3–4 times the initial length, i.e. at the limit, or even beyond that, of the range of the contractile apparatus (Van Mastrigt, 1988, figure 6), so that actine-myosine overlap was minimal. This view is supported by the disappearance of superimposed contractions at these cell lengths, so that in our opinion the passive behaviour in the end range of stretching must be attributed to structural changes in the cytoskeleton.

In accordance with the length dependence of  $dF$  the variables in Tables 3 and 4 point to length as the most reproducible parameter for predicting the sudden force decreases and ultimate breaking of the cells, whereas absolute force is a likely second candidate.

From Equation 7, based on the definition of the cell as a homogeneous (visco) elastic body, it follows that  $E$  is proportional to  $L^2 dF$ . As experiments show,  $dF$  is approximately proportional to length, so that  $E$  is approximately proportional to  $L^3$ . If on the other hand, it is the cyto-skeleton that bears the stress in the cells, this should probably be modelled as a bundle of thin wires, more or less orientated in parallel (Small *et al.*, 1986), so that a constant cross-section of the stress bearing filaments is a more likely assumption, leading to an elastic modulus proportional to  $LdF$  or to  $L^2$ . In both cases an elastic modulus increasing with length would result in agreement with our data.

Smooth muscle tissue, or more general soft tissue, has been generally known for a number of decades to exhibit increasing elastic moduli upon stretching (see for instance Remington, 1957; Fung, 1967; Ray, 1974). The urinary bladder wall forms no exception to this general rule (Coolsaet, 1975a; Susset & Regnier, 1981). Quantitatively, the dependence of the elastic modulus on strain was described by a mono-exponential function for strips of pig urinary bladder wall (Van Mastrigt *et al.*, 1978). The present data shows that the strain dependence in these tissues is not caused by connective tissue elements only, but that smooth muscle cells in isolation show comparable behaviour. In terms of magnitude, values calculated for  $E_{\text{max}}$  from pig bladder cells are found to be at least ten



times as high as  $E_{\max}$  for pig bladder strips (Van Mastrigt, 1977). This could imply that, in the intact tissue, the cells are interconnected with structures of a lower elastic modulus, e.g. elastin and reticulin. Generally, urinary bladder wall tissue consists of five components: smooth muscle cells, collagen, elastin, reticulin and ground substance. According to Fung (Fung, 1981) elastin shows the lowest-but-one elastic modulus of all soft tissue components. Smooth muscle in the passive state shows the lowest elastic modulus, whereas in the active state it has a very high elastic modulus. Collagen is very rigid, but in the intact tissue it is structurally folded in such a way that it does not contribute to the stress-strain relationship until the elastin and smooth muscle structures are considerably strained. Ground substance cannot bear much stress but its hydration state seems to modulate the behaviour of the other components (Van Duyl *et al.*, 1987; Fung, 1981). It seems that at different lengths in the intact tissue stress is borne to varying degrees by the different tissue components, which implies also a variation in the tissue's effective cross-sectional area: the tissue behaves as a fibre enforced composite material of low elasticity (Regnier *et al.*, 1989).

The interconnection of the smooth muscle cells by components of relatively low elasticity forms a plausible explanation for the higher  $E_{\max}$  found in single smooth muscle cells as compared to tissue strips. Another factor explaining the difference in  $E_{\max}$  might be found in the difference in actual cross-sectional area for the tissue modelled as a homogeneous body or as a bundle of filaments.

In our results force in both types of cells does not decrease to zero, at least not within the observation window of 80 s (see Tables 1 and 2, column 3). In all measurements, taken with increasing lengths, it was also either necessary to introduce a negative offset, or to change the A/D converter input sensitivity, to keep the peak force and the baseline level within the limits of the computer's maximum input range, which again indicates that cells did not relax to a zero level even after 15 min. In intact pig bladder strips (Van Mastrigt, 1977; Van Mastrigt *et al.*, 1978) only 26% of the initial force remained after 80 s of relaxation, whereas in the present data the fitted curves show an average remaining force of 84%. If all the bladder cell relaxation curves, including the non-fitted ones are taken into account, average remaining force after 80 s still yields 51%. Based on extrapolation of the one exponential model, the remaining force after

1000 s of relaxation would be 71%, which is considerably higher than the 17% measured after 1000 s of relaxation in intact bladder tissue strips (Van Mastrigt *et al.*, 1978). In the light of the complex structural arrangement of tissue components in the urinary bladder, as outlined previously, this difference can be explained by either a structural relaxation taking place, i.e. a rearrangement of the individual components (Alexander, 1957), or some of the non-muscular components showing a more viscous behaviour. These findings contrast with those of Van Dijk and coworkers (Van Dijk *et al.*, 1984) and Fay (1975), who find a stress relaxation to zero level within 30–120 s for bovine coronary and toad stomach smooth muscle cells respectively. As far as the findings of Van Dijk and coworkers are concerned, the decay to zero force level might be explained by slipping of the attachment which occurs, according to the same authors, at force levels above 1.5  $\mu\text{N}$ .

Although based upon morphological findings, one would expect uterus cells to be longer, and therefore to show a different length dependent behaviour compared with bladder cells, no significant differences between both types of cells were demonstrated in the present data. To what extent the differences in the occurrence of contractile phenomena in the relaxation curves between bladder and uterus cell are of importance will be discussed in a separate study.

In conclusion we state that:

- (1) Stress relaxation of urinary bladder single smooth muscle cells follows a pattern different from intact bladder tissue showing far less relaxation.
- (2) Stress relaxation of single smooth muscle cells of the pig urinary bladder and the human uterus does not continue to zero force, but levels off at a definite constant force level.
- (3)  $E_{\max}$  for single urinary bladder cells is at least a tenfold higher than was previously estimated from intact bladder tissue.
- (4) Passive properties of these cells are most likely determined by the cyto skeleton and the cell membrane.

### Acknowledgements

The authors wish to thank Professor Dr H. C. S. Wallenburg and Dr J. van Eijck from the department of Obstetrics and Gynaecology of the Dijkzigt Academic Hospital, Rotterdam, for kindly providing the uterus biopsies.

### References

- ALEXANDER, R. S. (1957) Elasticity of muscular organs. In: *Tissue Elasticity* (edited by REMINGTON, J. W.). Washington DC: American Physiology Society.
- COOLSAET, B. L. R. A. (1977) Stepwise cystometry. A new method to investigate properties of the urinary bladder. PhD Thesis. Rotterdam: Erasmus University, Rotterdam.
- COOLSAET, B. L. R. A., DUYL, W. A. VAN, MASTRIGT, R. VAN & SCHOUTEN, J. W. (1975a) Visco-elastic properties of bladder wall strips. *Inv. Urol.* **12**, 351–6.
- COOLSAET, B. L. R. A., DUYL, W. A. VAN, MASTRIGT, R. VAN & ZWART, A. VAN DER (1975b) Visco-elastic properties of the bladder wall. *Urol. Int.* **30**, 16–26.

- DIJK, A. M. VAN, WIERINGA, P. A., MEER, M. VAN DER & LAIRD, J. D. (1984) Mechanics of resting isolated single vascular smooth muscle cells from bovine coronary artery. *Am. J. Physiol.* **246**, C277–87.
- DOUGLAS, W. R. (1972) Of pigs and men and research. *Space Life Sci.* **3**, 226–34.
- DROGENDIJK, A. C., DUYL, W. A. VAN & ZON, A. T. M. VAN DER (1988) Provocation of contraction pikes of the cervix uteri by dilatation: Diagnostic significance for premature labour. In Proceedings of XII World Congress of Gynecology and Obstetrics, Rio de Janeiro, Brazil, October 23–28.
- DUYL, W. A. VAN, ZON, A. T. M. VAN DER, OOMENS, C. W. J. & DROGENDIJK, A. C. (1987) Stress relaxation, used as a tool for diagnosis of incompetence of human cervix in terms of a mixture model of tissue. In: *Biomechanics: Basic and Applied Research* (edited by BERGMAN, G., KOLBEL, R. & ROHLMANN, A.) pp. 193–8. Amsterdam: Martinus Nijhoff Publications.
- FAY, F. S. (1975) Mechanical properties of single isolated smooth muscle cells *INSERM*, **50**, 327–42.
- FUNG, Y. C. B. (1967) Elasticity of soft tissues in simple elongation. *Am. J. Physiol.* **213**, 1532–44.
- FUNG, Y. C. (1981) *Biomechanics: Mechanical Properties of Living Tissues*. Berlin and New York: Springer-Verlag.
- GLERUM, J. J. & MASTRIGT, R. VAN (1990a) Mechanical properties of mammalian single smooth muscle cells, part I: A low cost large range microforce transducer. *J. Musc. Res. Cell Motil.* **11**, 331–7.
- GLERUM, J. J. & MASTRIGT, R. VAN (1990b) Mechanical properties of mammalian single smooth muscle cells, part II: Evaluation of a modified technique for attachment cells to the measurement apparatus. *J. Musc. Res. Cell Motil.* **11**, 338–43.
- GLERUM, J. J., MASTRIGT, R. VAN, ROMIJN, J. C. & GRIFFITHS, D. J. (1987) Isolation and individual electrical stimulation of single smooth-muscle cells from the urinary bladder of the pig. *J. Musc. Res. Cell Mot.* **8**, 125–34.
- GOSLING, J. A., DIXON, J. S. & HUMPHERSON, J. R. (1983) *Functional Anatomy of the Urinary Tract*. pp. 3.16–18. London and New York: Gower Medical Publishing.
- HAI, C. M. & MURPHY, R. A. (1988a) Cross-bridge phosphorylation and regulation of latch state in smooth muscle. *Am. J. Physiol.* **254**, C99–106.
- HAI, C. M. & MURPHY, R. A. (1988b) Regulation of shortening velocity by cross-bridge phosphorylation in smooth muscle. *Am. J. Physiol.* **255**, C86–94.
- HAM, A. W. (1974) *Histology*. 7th edition. pp 869–70. Philadelphia and Toronto: J. B. Lippincott Company.
- KIRKEGAARD, D. (1970) *A Fortran IV Version of the Sum-of-Exponential Least Squares Code Exposum*. Riso: Danish Atomic Energy Commission, Research Establishment.
- KONDO, A. & SUSSET, J. G. (1972) Cystometrie rapide-principe et application clinique. *L'union Med. du Can.* **101**, 1141–5.
- LEVIN, R. M., RUGGIERI, M. R., VELAGAPUDI, S., GORDON, D., ALTMAN, B. & WEIN, A. J. (1986) Relevance of spontaneous activity to urinary bladder function: an *in vitro* and *in vivo* study. *J. Urol.* **136**, 517–21.
- MARSTON, S. B. (1989) What is latch? New ideas about tonic contraction in smooth muscle. *J. Musc. Res. Cell Mot.* **10**, 97–100.
- RAY, C. D. (1974) *Medical Engineering*. pp. 199–215, 558–66. Chicago: Year Book Publishers.
- REGNIER, C. H., MEYER, S., SUSSET, J. G. & ELBADAWI, A. (1989) Biomechanical/microstructural basis of bladder compliance: A model proposal, and a preliminary experimental study. In *Proceedings of the Urodynamics Society, Texas, USA, May 6, 1989*.
- REMINGTON, J. W. (1957) Extensibility behaviour and hysteresis phenomena in smooth muscle tissues. In *Tissue Elasticity* (edited by REMINGTON, J. W.). Washington DC: American Physiology Society.
- SMALL, J. V., FÜRST, D. O. & MEY, J. de (1986) Localization of filamin in smooth muscle. *J. Cell Biol.* **102**, 210–20.
- SQUIRE, J. (1981) *The Structural Basis of Muscular Contraction*. pp. 443–61. New York and London: Plenum Press.
- STEPHENS, N. L. (1984) *Smooth Muscle Contraction*. New York and Basel: Marcel Dekker Inc.
- SUSSET, J. G. & REGNIER, C. H. (1981) Viscoelastic properties of bladder strips. Standardization of a technique. *Inv. Urol.* **18**, 445–50.
- VAN MASTRIGT, R. (1977) A systems approach to the passive properties of the urinary bladder in the collection phase. PhD Thesis, Erasmus University, Rotterdam, pp 80–95. Delft: Delft University Press.
- VAN MASTRIGT, R. (1988) The length dependence of the series elasticity of pig bladder smooth muscle. *J. Musc. Res. Cell Mot.* **9**, 525–32.
- VAN MASTRIGT, R. (1989) The force recovery following repeated quick releases applied to pig urinary bladder smooth muscle. *J. Musc. Res. Cell Mot.*, submitted for publication.
- VAN MASTRIGT, R., COOLSAET, B. L. R. A. & DUYL, W. A. VAN (1978) Passive properties of the urinary bladder in the collection phase. *Med. & Biol. Eng. & Comput.* **16**, 471–82.
- VAN MASTRIGT, R., COOLSAET, B. L. R. A. & DUYL, W. A. VAN (1981) First results of stepwise straining of the human urinary bladder and human bladder strips. *Inv. Urol.* **19**, 58–61.
- ZON, A. T. M. VAN DER, DUYL, W. A. VAN & DROGENDIJK A. C. (1989) Measurement of cervical relaxation: A new diagnostic tool for cervical incompetence. *Obstet. and Gynec.*, submitted for publication.